Diagnosis toward predicting mean annual runoff in ungauged basins

Yuan Gao, Lili Yao, Ni-Bin Chang and Dingbao Wang*

Department of Civil, Environmental, and Construction Engineering, University of Central Florida, Orlando, FL 32816, United States

*Correspondence to D. Wang, dingbao.wang@ucf.edu

Abstract

Prediction of mean annual runoff is of great interest but still poses a challenge in ungauged basins. The present work diagnoses the prediction in mean annual runoff affected by the uncertainty in estimated distribution of soil water storage capacity. Based on a distribution function, a water balance model for estimating mean annual runoff is developed, in which the effects of climate variability and the distribution of soil water storage capacity are explicitly represented. As such, the two parameters in the model have explicit physical meanings, and relationships between the parameters and controlling factors on mean annual runoff are established. The estimated parameters from the existing data of watershed characteristics are applied to 35 watersheds. The results showed that the model could capture 88.2% of the actual mean annual runoff on average across the study watersheds, indicating that the proposed new water balance model is promising for estimating mean annual runoff in ungauged watersheds. The underestimation of mean annual runoff is mainly caused by the underestimation of the area percentage of low soil water storage capacity due to neglecting the effect of land surface and bedrock topography. Higher spatial variability of soil water storage capacity estimated through the Height Above the Nearest Drainage (HAND) and Topographic Wetness Index (TWI) indicated that topography plays a crucial role in determining the actual soil water storage capacity. The performance of mean annual runoff prediction in ungauged basins can be improved by employing better estimation of soil water

storage capacity including the effects of soil, topography, and bedrock. It leads to better diagnosis of the data requirement for predicting mean annual runoff in ungauged basins based on a newly developed process-based model finally.

Keywords: mean annual runoff; ungauged; storage capacity; curve number; soil; topography; bedrock

1. Introduction

Hydrologists have a long-standing interest in mean annual water balance modeling and prediction. The factors controlling mean annual runoff have been studied in literature. Mean climate has been identified as the first order control on mean annual runoff and evaporation and it has been quantified by climate aridity index, which is defined as the ratio between the mean annual potential evapotranspiration (E_p) and precipitation (P) (Turc, 1954; Pike, 1964). Other controlling factors include the temporal variability of climate (Farmer et al., 2003; Troch et al., 2002; Fu and Wang, 2019), vegetation (Zhang et al., 2001; Donohue et al., 2007; Gentine et al., 2012; Li et al., 2013), soil (Atkinson et al., 2002; Yokoo et al., 2008; Li et al., 2014), and topography (Woods, 2003; Abatzoglou and Ficklin, 2017). Mean annual runoff or evaporation has been modeled as a function of climate aridity index and the equation is usually called as Budyko equation (Budyko, 1958). The effects of other factors are represented by including a parameter to Budyko equation (Fu, 1981; Yang et al., 2008; Wang and Tang, 2014). Among these factors, climate including its mean and temporal variability, and soil water storage capacity including its mean and spatial variability are dominant catchment characteristics controlling mean annual runoff, especially for those catchments dominated by saturation excess runoff generation (Milly, 1994).

Intra- and inter-annual climate variability introduces non-steady state conditions to finer timescale water balances and the non-steady state effect could propagate to the mean annual runoff. The effects of seasonal variations of precipitation and potential evaporation on long-term runoff have been studied in several studies. Milly (1994) showed that seasonality tends to increase mean annual runoff through a stochastic soil moisture model. The seasonality effects have been demonstrated through a top-down model by Hickel and Zhang (2006) and a classification study by Berghuijs et al. (2014). Mean annual water balance also receives impacts from climate variability at the inter-annual and daily timescales. Li (2014) showed that the inter-annual variability of precipitation and potential evaporation could increase the mean annual runoff up to 10% based on a stochastic soil moisture model. Shao et al. (2012) found that daily precipitation with a larger variation potentially increases mean annual runoff especially in the catchments where infiltration excess runoff is prevalent. Yao et al. (2020) quantified the relative contribution of daily, monthly and inter-annual climate variabilities to mean annual runoff and showed that the contribution decreases, by average, from monthly to inter-annual scale, and then daily scale.

Soil water storage capacity is the maximum storage capacity from land surface to bedrock, which exerts a powerful control on mean annual runoff (Konapala and Mishra, 2016). A smaller soil water storage capacity creates favorable conditions for runoff generation because the precipitation in excess of the available storage capacity would be lost as runoff directly, while catchments with a lager soil water storage capacity could hold more precipitation for evaporation (Sankarasubramanian and Vogel, 2002; Porporato et al., 2004; Chen et al., 2013). Soil water storage capacity is closely related to vegetation since the root structure of vegetation could affect soil water storage capacity significantly. Research has been conducted to reveal the role of soil water storage capacity through the linkage of vegetation and model parameter (Yang et al., 2008;

Chen and Wang, 2015). Gerrits (2009) developed equations for transpiration and interception by considering the root zone and interception storage capacity as two of the most important catchment characteristics affecting evapotranspiration. In addition to the magnitude of the average soil water storage capacity, the spatial variability of soil water storage capacity within a catchment also influences precipitation partitioning at the event scale, and further influences the cumulative runoff at the mean annual scale (Moore, 1985; Jothityangkoon et al., 2001; Gao et al., 2016). It has also been suggested that the spatial variability of soil water storage capacity could suppress the actual evaporation because the maximum evaporation in areas with soil water storage capacity less than E_p will be smaller than E_p; therefore, the average evaporation over the entire catchment is smaller than E_p even though the average storage is greater than E_p, resulting in more runoff generation compared to the situation when the soil water storage capacity is spatially uniform (Yao et al., 2020).

Therefore, climate variability and soil water storage capacity need to be explicitly incorporated into the model for predicting mean annual runoff. The effect of climate variability could be taken into account by driving the model with daily precipitation and potential evaporation which are usually available. The spatial distribution of soil water storage capacity could be modelled by a distribution function, and it is usually modelled by the generalized Pareto distribution (Moore, 1985; Zhao, 1992). The distribution function includes two parameters, i.e., the shape parameter and the maximum storage capacity over the watershed. In ungauged basins, soil water storage capacity and its spatial variability need to be estimated directly from available data. Gao et al. (2014) adopted the mass curve technique, which has been used for designing the storage capacity of reservoir, to estimate the average water storage capacity of the root zone using precipitation and potential evaporation data. The shape parameter of the distribution function has

been estimated from soil data (Huang et al., 2003). However, the estimated parameters from these methods bring much uncertainty in runoff estimation, and the two parameters of the generalized Pareto distribution are usually estimated by model calibration using observed streamflow data (Wood et al., 1992; Alipour and Kibler, 2018, 2019).

The objective of this paper is to develop a nonparametric mean annual water balance model for predicting mean annual runoff in ungauged basins, which has not yet been fully understood (Blöschl et al., 2013). The mean annual water balance model is forced by daily precipitation and potential evaporation; therefore, the climate variability at different timescales is represented explicitly in the climate input. The runoff generation is quantified by a distribution function for describing the spatial distribution of soil water storage capacity (Wang, 2018). The mean and the shape parameter of the distribution function need to be estimated from the available data in ungauged basins. Therefore, the model serves as a diagnosis tool for evaluating the data requirement for estimating soil water storage capacity. The mean soil water storage capacity is estimated from curve number and climate because soil water storage capacity consists of the antecedent soil water storage and the potential maximum soil moisture retention which can be calculated through SCS curve number method. The estimation of the shape parameter is diagnosed in terms of the data requirement including soil, land surface topography, and bedrock topography. Section 2 introduces the new mean annual water balance model and the study watersheds. Results and discussion are presented in Section 3, followed by Section 4 for conclusions.

2. Methodology

2.1 Mean annual runoff model

Climate variability is defined as the temporal variations of precipitation (P) and potential evapotranspiration (E_p), including their intra-monthly, intra-annual, and inter-annual variations.

For example, the deviations of daily P or E_p from its monthly mean values are defined as the intra-monthly variations (Yao et al., 2020). As discussed in the introduction section, the mean annual runoff model takes daily precipitation and potential evaporation as inputs, therefore, climate variability is explicitly included in the model. The developed model calculates daily soil wetting (infiltration) and evaporation by tracking the soil water storage. Mean annual runoff is estimated by aggregating the daily values. The daily soil wetting is calculated using the concept of saturation excess runoff generation by modeling the spatial variability of soil moisture and soil water storage capacity. To facilitate the parameter estimation of storage capacity distribution in ungauged basins, the following distribution function is used for modeling the spatial distribution of storage capacity (Wang, 2018):

$$F(C) = 1 - \frac{1}{a} + \frac{C+(1-a)S_b}{a\sqrt{(C+S_b)^2-2aS_bC}} \quad (1)$$

where $F(C)$ is the cumulative distribution function (CDF), representing the fraction of the watershed area for which the soil water storage capacity is equal to or less than C; a is the shape parameter of the distribution and varies between 0 and 2; and S_b is the average soil water storage capacity over the watershed (i.e., the mean of the distribution). As shown in Wang (2018), this distribution function leads to the SCS curve number (SCS-CN) method when the initial storage is set to zero. Therefore, there is a linkage between S_b and the "potential maximum retention after runoff begins" in the SCS-CN method, denoted as S_{CN}.

Daily soil wetting and runoff generation is computed as a function of daily precipitation (P), initial storage (S_0), a, and S_b. As shown in Wang (2018), the average soil wetting (W) is computed by:

$$W = \frac{P+S_b\sqrt{(m+1)^2-2am}-\sqrt{[P+(m+1)S_b]^2-2amS_b{}^2-2aS_bP}}{a} \quad (2)$$

where $m = \frac{S_0(2S_b - aS_0)}{2S_b(S_b - S_0)}$. Setting $S_0 = 0$ and dividing P on both sides of Equation (2), a Budyko-type equation, representing $\frac{W}{P}$ as a function of $\frac{S_b}{P}$, is obtained (Wang and Tang, 2014), which has been used to model long-term soil wetting (Tang and Wang, 2017). Therefore, Equation (2) can be interpreted as a non-steady state Budyko equation which accounts for the effect of water storage. Daily evaporation (E_d) is computed as (Yao et al., 2020):

$$E_d = \frac{W + S_0}{S_b} \frac{E_p + S_b - \sqrt{(E_p + S_b)^2 - 2aS_bE_p}}{a} \quad (3)$$

The first component on the right-hand side of Equation (3), $\frac{W+S_0}{S_b}$, is the percentage of storage, and the second component is the evaporation for the condition when the entire watershed is saturated, i.e., the spatial distribution of soil water storage is same as that of storage capacity (Yao et al., 2020). Dividing $W + S_0$ on both-hand sides, Equation (3) represents $\frac{E_d}{W+S_0}$ as a function of $\frac{E_p}{S_b}$, and the function is same as the Budyko-type equation derived by Wang and Tang (2014). Mean annual evaporation ($\bar{E}$) is computed by aggregating the daily evaporation, and mean annual runoff ($\bar{Q}$) is computed as the difference of mean annual precipitation and evaporation:

$$\bar{E} = \frac{\sum_{y=1}^{Y} \sum_{d=1}^{D_y} E_d}{Y} \quad (4)$$

$$\bar{Q} = P - \bar{E} \quad (5)$$

where, Y is the number of years, and D_y is the number of days in yth year; y and d represent the yth year and d^{th} day, respectively. Note that the mean annual runoff includes surface runoff and baseflow, and both are impacted by climate variability (e.g., intra-annual variability) (Berghuijs et al., 2014; Fan et al., 2007).

This mean annual water balance model applies two non-steady Budyko-type equations at the daily scale, one for daily soil wetting and the other for daily evaporation. Runoff routing is

not necessary since the model is prepared for long-term water balance analysis. As a result, the mean annual water balance model includes two parameters, i.e., the shape parameter (a) and the average soil water storage capacity (S_b). For studies where a one-parameter Budyko equation is applied to long-term scale directly, the effects of climate variability (seasonality, inter-annual variability, and daily storminess) on mean annual water balance are attributed to the single parameter of Budyko equation (e.g., Fu, 1981; Zhang et al., 2001). This creates the challenge to estimate the single parameter in ungauged basins; whereas, the mean annual water balance model used in this paper takes daily precipitation and potential evaporation as inputs, and the effects of climate variability are taken into account explicitly. To achieve the goal of predicting mean annual runoff in ungauged basins, a and S_b need to be estimated in ungauged basins.

2.2 Parameter estimation

2.2.1 Average soil water storage capacity

Under a given soil moisture condition, soil water storage capacity is the sum of actual water storage and the remaining (or effective) storage capacity. The effective storage capacity corresponding to the normal antecedent moisture condition defined in the SCS-CN method, S_{CN} (mm), is computed as a function of CN (SCS, 1972; Bartlett et al., 2016):

$$S_{CN} = 25.4(1000/CN - 10) \quad (6)$$

where CN is the composite curve number based on land use and land cover (LULC) and hydrologic soil group (HSG) for each watershed. The LULC data can be obtained from the National Land Cover Database (Homer et al., 2015), and the HSG data can be extracted from the Gridded Soil Survey Geographic (gSSURGO) database with a spatial resolution of 10 m (*USDA*, 2014). In HSG, soils are assigned to one of the four groups (A, B, C, and D) and three dual classes (A/D, B/D, and C/D) according to the rate of infiltration when the soils are not protected by vegetation

and receive precipitation from long-duration storms. For the cells characterized by dual classes, the CN value is calculated as the average of the two CN values corresponding to the two soil groups.

The average soil water storage capacity (S_b) is the sum of the actual storage under the normal condition ($\bar{S}$) and its corresponding effective storage capacity:

$$S_b = \bar{S} + S_{CN} \tag{7}$$

The physical meaning of S_b is the mean value of the soil water storage capacity over a watershed which is defined as the maximum storage from land surface to bedrock in this study rather than the storage capacity from shallow soils. Since the "normal antecedent moisture" can be interpreted as the steady-state soil moisture condition, $\bar{S}$ is the long-term average storage over the watershed. The values of $\bar{S}$ for 59 MOPEX (MOdel Parameter Estimation Experiment) watersheds are estimated based on the long-term water balance model in Yao et al. (2020); and these watersheds do not include any watersheds studied in this paper. The long-term water balance model used in their study has a same model structure but the two parameters, i.e., the mean value of the soil water storage capacity and its shape parameter in the distribution function, were obtained by model calibration. The ratio between $\bar{S}$ and S_b is defined as the long-term storage ratio $\left(\frac{\bar{S}}{S_b}\right)$. It is found that the values of $\frac{\bar{S}}{S_b}$ for all the watersheds were larger than 0.5. As shown in Figure 1, $\frac{\bar{S}}{S_b}$ has a linear relationship with the climate aridity index:

$$\frac{\bar{S}}{S_b} = -0.46\Phi + 1.2 \tag{8}$$

where Φ is the climate aridity index. Substituting Equations (6) and (7) into Equation (8), one can estimate the average soil water storage capacity as a function of curve number and climate aridity index:

$$S_b = \frac{S_{CN}}{0.46\Phi - 0.2} \quad (9)$$

2.2.2 Shape parameter

The spatial variability of storage capacity is determined by the spatial distribution of point-scale pore space across the watershed. The volume of soil pores at point scale can be determined by soil thickness and porosity in different soil layers. The porosity (θ_s) for each layer is calculated from the soil bulk density:

$$\theta_s(j) = 1 - \frac{\rho_b(j)}{\rho} \quad (10)$$

where j denotes the j^{th} soil layer; $\rho_b(j)$ is the bulk density of the j^{th} soil layer; ρ is the particle density (2.65 g/cm^3). After obtaining the porosity, the point-scale storage capacity can be calculated as the following equation (Huang et al., 2003):

$$C = \sum_1^n z_j \cdot \theta_s(j) \quad (11)$$

where C is the point-scale soil storage capacity; n is the number of soil layers; z_j and $\theta_s(j)$ are the thickness and porosity of the j^{th} soil layer, respectively. In the gSSURGO database, the soil thickness and bulk density for each layer are available for shallow soil from the land surface to ~ 2 m soil depth.

The total soil thickness at each point is the elevation difference from land surface to fresh bedrock. However, the bedrock topography is difficult to obtain especially at the watershed scale. Alternatively, it is assumed that the spatial distribution of the actual soil water storage capacity is same as the spatial distribution of water storage capacity computed from the gSSURGO database. In order to compare the shape parameter evaluated from the soil data with its counterparts evaluated from other methods, the point-scale storage capacity is normalized with the average storage capacity over the watershed, and Equation (1) is rewritten as:

$$F(x) = 1 - \frac{1}{a} + \frac{x+(1-a)}{a\sqrt{(x+1)^2-2ax}} \quad (12)$$

where x is the normalized storage capacity $\left(\frac{C}{S_b}\right)$ at point scale; a is the shape parameter describing the spatial variability of soil water storage capacity. The shape parameter a is then estimated by fitting the point-scale storage capacity data obtained from Equation (11). A nonlinear programming solver using derivative-free method (i.e., Matlab function "fminsearch") was used to calculate the optimal shape parameter by minimizing the root mean square error (RMSE). To demonstrate the sensitivity of mean annual runoff to the value of shape parameter, Figure 2 presents mean annual runoff versus shape parameter based on the mean annual water balance (Yao et al., 2020). It can be found that mean annual runoff decreases significantly as the shape parameter increases, especially when shape parameter approaches its upper limit (i.e., 2). The negative relationship between the mean annual runoff and the shape parameter can be attributed to the fact that the larger shape parameter indicates that less watershed area has small values of point-scale storage capacity (Wang, 2018) and more precipitation could be retained underground for evaporation.

2.3. Study watersheds

The estimations of mean annual runoff in 35 watersheds are diagnosed in this paper. The number of 35 was determined due to the consideration of the data availability including soil (hydrologic soil group), land cover and land use, DEM as well as the minimum snow effect and human activities (Wang and Hejazi, 2011), and to keep the efforts of gSSURGO data processing to a reasonable level while still to have a sufficient number of sample of watersheds. The drainage area of the watersheds varies from 2044 to 9889 km^2. Table 1 shows the USGS gauge number and climate aridity index of these watersheds. The saturation excess is the dominated runoff generation

247 in these watersheds. Daily precipitation and streamflow data during 1948 – 2003 are extracted
248 from the MOPEX dataset (Duan et al., 2006), and the daily potential evaporation during this period
249 is calculated based on the Hargreaves method (Hargreaves and Samani, 1985) by using the daily
250 maximum, minimum, and mean temperature. The average soil water storage capacity and the
251 shape parameter for these watersheds are estimated from the available data of climate, LULC, soil,
252 and topography, and the predictions of mean annual runoff are diagnosed.

253 **3. Results and discussion**

254 **3.1. Estimated average soil water storage capacity**

255 The potential maximum retention (S_{CN}) is calculated based on the average CN in each
256 watershed (Table 1). The average CN is computed based on LULC and hydrologic soil group.
257 For examples, Figure 3a shows the LULC map for the Fox River watershed in Wisconsin and
258 Figure 3d shows the LULC map for the Spoon River watershed in Illinois. The dominant land
259 uses are agriculture (49%) and forest (33%) in the Fox River watershed, and agriculture (77%) and
260 forest (15%) in the Spoon River watershed. The hydrologic soil groups are shown in Figure 3b
261 (Fox River watershed) and Figure 3e (Spoon River watershed). Given the same LULC, the
262 hydrologic soil group D is more favorable for runoff generation compared with group A. The
263 dominant hydrologic soil groups are group A (31%) and group B (19%) in the Fox River watershed,
264 and group C/D (49%) and group B/D (20%) in the Spoon River watershed. The calculated CN for
265 each grid cell is shown in Figure 3c (Fox River watershed) and Figure 3f (Spoon River watershed).
266 The average CN is 61.0 for the Fox River watershed and 78.1 for the Spoon River watershed.
267 Since the Spoon River watershed has a higher percentage of agricultural land and lower soil
268 permeability, its average CN is higher than that for the Fox River watershed. Correspondingly,
269 the calculated S_{CN} in the Fox River watershed (162 mm) is higher than that in Spoon River

watershed (71 mm). The values of S_{CN} over the study watersheds vary from 56 mm (Auglaize River watershed) to 182 mm (Chattahoochee River watershed) as shown in Table 1.

The average soil water storage capacity is estimated based on the computed S_{CN} and climate aridity index shown in Equation (8). For examples, the climate aridity index in the Fox River watershed is 1.12 which is the same as that in the Spoon River watershed. The estimated S_b is 721 mm in the Fox River watershed and 314 mm for the Spoon River watershed. As shown in Table 1, the estimated S_b varies from 177 mm (Chikaskia River watershed) to 1559 mm (Chattahoochee River watershed) over the study watersheds. Figure 4a shows the spatial distribution of the estimated S_b. Watersheds with higher S_b are mostly distributed in the eastern US, where the aridity index is relatively lower than that in the other watersheds.

3.2. Estimated shape parameter

The shape parameter (a) for the distribution of soil water storage capacity is estimated based on the soil data in the gSSURGO database. For examples, the black circles in Figure 5 show the normalized storage capacity for the Fox River watershed (Figure 5a) and the Spoon River watershed (Figure 5b) based on the soil data in the gSSURGO database. As shown in Figure 5, the normalize CDF for both watersheds shows an S-shape. The estimated shape parameter is 1.996 for the Fox River watershed (RMSE = 0.58) and 1.990 for the Spoon River watershed (RMSE = 1.27) by fitting to the soil data. Higher value of shape parameter indicates less spatial variability; therefore, the spatial variability in the Spoon River watershed is higher than that in the Fox River watershed. The mean value of RMSE for the 35 study watersheds is 0.06. Figure 4b shows the estimated shape parameters for the study watersheds, which vary from 1.830 to 1.998.

3.3. Diagnosing mean annual runoff prediction

The estimated values of S_b and a based on climate, LULC, and soil data are applied to the mean annual water balance model. The comparison of simulated and observed mean annual runoff for the study watersheds is shown in Figure 6a. The RMSE for estimated mean annual runoff is 80 mm/yr. The water balance model captures 88.2% of the mean annual runoff across the 35 study watersheds; therefore, the methods for estimating S_b and a based on the available data are promising for predicting annual runoff in ungauged basins.

The water balance model with the estimated values of S_b and a underestimates the mean annual runoff in some watersheds, and the relative underestimation error is 11.8% on average among all the study watersheds. The underestimation of mean annual runoff could be due to the biased estimation of the shape parameter. As described in Section 3, the spatial variability of soil water storage capacity is assumed to be equal with the spatial variability of the pore space in the shallow soil. The pore space at the point scale is calculated through the porosity and soil thickness. The thickness of the shallow soil in the gSSURGO database is quite uniformly distributed across the watershed, i.e., around 2 m; whereas, the actual soil thickness including the weathered bedrock is the elevation difference between the land surface and fresh bedrock, and can be highly heterogeneous due to the variable land surface and bedrock topography over the watershed.

To diagnose the effect of land surface and bedrock topography on mean annual water balance, the shape parameter is calibrated using the observed streamflow. The streamflow data during 1948-2003 are divided into three periods: 1) the warm-up period (1948-1953); 2) the calibration period (1954-1973); and 3) the validation period (1974-2003). During the calibration, the estimated S_b based on CN is used, and a is the only free parameter to be calibrated. The calibration is conducted by minimizing the absolute error of the observed and simulated mean annual runoff through a global optimization method, i.e., Shuffled Complex Evolution Method

315 (Duan et al., 1992). As shown in Figure 6b, most of the calibrated a are smaller than the estimated
316 a based on soil data only. The performance of predicted mean annual runoff (during the validation
317 period) is improved with the calibrated shape parameter (Figure 6c). The average of absolute error
318 for the mean annual runoff is 7.1%.

319 The overestimation of shape parameter based on the soil porosity data underestimates the
320 area percentage of low soil water storage capacity compared with the calibrated one as shown in
321 Figure 5a for the Fox River watershed and Figure 5b for the Spoon River watershed. The slope at
322 the normalized soil water storage capacity around 1 for the estimated shape parameter is higher
323 than that for the calibrated one. Therefore, the calibrated shape parameter indicates a larger spatial
324 variability. The underestimation of catchment area with low soil water storage capacity could be
325 resulted from neglecting the effect of land surface and bedrock topography which cannot be
326 referred from the soil database (gSSURGO) where the point-scale soil thickness is around 2 m.

327 To explore the impact of land surface topography on the spatial distribution of soil water
328 storage capacity, the soil data (i.e., porosity) is combined with the Height Above the Nearest
329 Drainage (HAND) method proposed by Gao et al. (2019). HAND is the vertical elevation
330 difference from a point to its nearest drainage point. The distribution of HAND was used for
331 estimating the shape parameter of the spatial distribution of storage capacity. Therefore, the
332 HAND method uses land surface topography data only for estimating the shape parameter. In our
333 analysis, the porosity of the soil beyond the bottom layer in the soil database is assigned with the
334 same value as the bottom layer. For example, if the HAND for a grid cell is 10.0 m and the porosity
335 and depth of the bottom soil layer in the gSSURGO database is 0.2 and 2.0 m, respectively, the
336 porosity for the soil from 2.0 m to 10.0 m depth is assigned with 0.2. Finally, the total volume of

pores is calculated for each grid cell based on the soil porosity obtained from the gSSURGO database and the HAND value based on land surface topography.

The control of land surface topography on the hydrologic process has also been widely quantified through topographic wetness index (TWI) of TOPMODEL (Beven and Kirkby, 1979). The spatial variability of soil storage capacity based on the TOPMODEL assumption has been demonstrated as a beneficial representation of the conceptual model (Sivapalan et al., 1997). Therefore, the heterogeneity of TWI in a watershed was proposed to be another surrogate of the heterogeneity of the soil storage capacity in this study, and the shape parameter estimated by fitting TWI against Equation (12) through minimizing the root mean square error (RMSE) for the Maquoketa River in Iowa was compared with those obtained from other methods.

The dashed blue line in Figure 7 shows the porosity-HAND based CDF of normalized soil water storage capacity for the Maquoketa River in Iowa (gauge #05418500). The stream initiation threshold used for calculating HAND is 40 km^2 which is 1% of the maximum flow accumulation (Maidment, 2002). The threshold affects the value of HAND but this is beyond the scope of this paper. The best fit value of a for the porosity-HAND based CDF is 1.779, which overestimates the spatial variability of storage capacity compared with the calibrated shape parameter (a=1.905). This is due to the assumption of the HAND method that the bedrock between a specific point and its nearest drainage point is horizontal and intercepts with the channel bed. However, the bedrock topography may have various slopes in a watershed (Troch et al., 2002). Therefore, the true value of a (indicated by the calibrated one) potentially falls between the a obtained from soil data and the a based on soil and HAND. The bedrock topography from observation or models is needed to accurately estimate the shape parameter. The dashed dot red line in Figure 7 displays the CDF of the normalized soil storage capacity based on TWI, and the corresponding value of a is 1.967. The

TWI-based a value also presents a larger spatial variability than that derived from soil data solely, confirming the importance of topography in determining the heterogeneity of soil water storage capacity. The deviation of the TWI-based a value from its calibrated counterpart could be due to the fact that the bedrock topography is not considered in TWI.

4. Conclusion

A mean annual water balance model based on the concept of saturation excess runoff generation is used for diagnosing the potential for nonparametric modeling of mean annual runoff in ungauged basins. The model takes the effect of climate variability into account explicitly since it is driven by daily precipitation and potential evapotranspiration at the daily time step. The distribution function, which leads to the SCS curve number method, is used for describing the spatial distribution of soil water storage capacity. The mean (i.e., average soil water storage capacity) and the shape parameter (i.e., the spatial variability of soil storage capacity over the watershed) of the distribution function can be estimated from the available data. Based on the linkage of the distribution function and the SCS curve number method, a new method based on the existing observed data of watershed characteristics is proposed for estimating the average soil water storage capacity. The average soil water storage capacity (S_b), as one of the parameters in the model, was estimated as a function of climate aridity index and curve number which is calculated based on land cover and soil data.

The developed mean annual water balance was applied to diagnose the estimation of shape parameter (a) in this study. The shape parameter, describing the spatial variation of soil water storage capacity, was first estimated based on the porosity and soil thickness data in the soil database (gSSURGO). The estimated values of a were tested in 35 watersheds. The results showed that the model with the estimated values of S_b and a underestimated the mean annual

runoff by 11.8% on average over all the study watersheds. The underestimation of runoff is mainly caused by the underestimation of the spatial heterogeneity of soil thickness over the watershed. The Height Above the Nearest Drainage (HAND) was then calculated as the total soil thickness for estimating the total volume of the pore space. The result showed that topography is of great importance for determining the spatial variability of soil water storage capacity. The estimated shape parameter from porosity-HAND overestimated the spatial variability of the storage capacity compared with the calibrated a, which may result from the assumed bedrock in the HAND method. The Topographic Wetness Index (TWI) based shape parameter further indicated the importance the topography including the land surface topography and bedrock topography. Future research will investigate alternative methods for better estimating the spatial variability of soil water storage capacity over watersheds, and quantify the impacts of vegetation and climate variability (e.g., distribution of rainy days, the magnitude and the seasonality of climate variables).

Data availability

The soil and land use and land cover data that support the findings of this study are openly available at: https://websoilsurvey.sc.egov.usda.gov/App/WebSoilSurvey.aspx (Natural Resources Conservation Services, United States Department of Agriculture), and: https://www.mrlc.gov/data?f%5B0%5D=category%3Aland%20cover&f%5B1%5D=region%3Aconus (National Land Cover Database, United States Geological Survey), respectively. Daily precipitation, streamflow, and temperature data are available from 1948 to 2003 through the MOPEX website at https://hydrology.nws.noaa.gov/pub/gcip/mopex/US_Data/.

Author contributions

Dingbao Wang designed the study, contributed to the methods, results discussion and modified the text. Yuan Gao quantified the parameters of the model and prepared the manuscript with contributions from all co-authors. Lili Yao developed the model code, quantified the parameters, performed the simulations and prepared the manuscript with contributions from all co-authors. Ni-Bin Chang contributed to the introduction and modified the text.

Competing interests

The authors declare that they have no conflict of interest.

Acknowledgements

This research was funded in part under award CBET-1804770 from National Science Foundation (NSF) and Florida Department of Transportation (FDOT).

Reference

Abatzoglou, J. T., and Ficklin, D. L.: Climatic and physiographic controls of spatial variability in surface water balance over the contiguous United States using the Budyko relationship, Water Resour. Res., 53(9), 7630-7643, https://doi.org/10.1002/2017WR020843, 2017.

Alipour, M. H. and Kibler, K. M.: A framework for streamflow prediction in the world's most severely data-limited regions: test of applicability and performance in a poorly-gauged region of China, J. Hydrol., 557, 41-54, https://doi.org/10.1016/j.jhydrol.2017.12.019, 2018.

Alipour, M. H. and Kibler, K. M.: Streamflow prediction under extreme data scarcity: a step toward hydrologic process understanding within severely data-limited regions, Hydrolog. Sci. J., 64(9), 1038-1055, https://doi.org/10.1080/02626667.2019.1626991, 2019.

Atkinson, S. E., Woods, R. A., and Sivapalan, M.: Cimate and landscape controls on water balance model complexity over changing timescales, Water Resour. Res., 38(12), 1314, https://doi.org/10.1029/2002WR001487, 2002.

Bartlett, M. S., Parolari, A. J., McDonnell, J. J., and Porporato, A.: Beyond the SCS-CN method: A theoretical framework for spatially lumped rainfall-runoff response, Water Resour. Res., 52(6), 4608-4627, https://doi.org/10.1002/2015WR018439, 2016.

Berghuijs, W. R., Sivapalan, M., Woods, R. A., and Savenije, H. H.: Patterns of similarity of seasonal water balances: A window into streamflow variability over a range of time scales, Water Resour. Res., 50(7), 5638-5661, https://doi.org/10.1002/2014WR015692, 2014.

Beven, K. J. and Kirkby, M. J.: A physically-based variable contributing area model of basin hydrology. Hydrolog. Sci. J., 24(1), 43-69, 1979.

Blöschl, P. G., Sivapalan, P. M., Wagener, P. T., Viglione, D. A., and Savenije, H. H.: Runoff Prediction in Ungauged Basins: Synthesis across Processes, Places and Scales, Cambridge Univ. Press, Cambridge, U. K., 2013.

Budyko, M.I.: The Heat Balance of the Earth's Surface, U.S. Dep. of Commer., Washington, D. C., 1958.

Chen, X., Alimohammadi, N., and Wang, D.: Modeling interannual variability of seasonal evaporation and storage change based on the extended Budyko framework, Water Resour. Res., 49(9), 6067-6078, https://doi.org/10.1002/wrcr.20493, 2013.

Chen, X. and Wang, D.: Modeling seasonal surface runoff and base flow based on the generalized proportionality hypothesis, J. Hydrol., 527, 367-379, https://doi.org/10.1016/j.jhydrol.2015.04.059, 2015.

Donohue, R. J., Roderick, M. L., and McVicar, T. R.: On the importance of including vegetation dynamics in Budyko's hydrological model, Hydrol. Earth Syst. Sci., 11, 983-995, https://doi.org/10.5194/hess-11-983-2007, 2007.

Duan, Q., Sorooshian, S., and Gupta, V.: Effective and efficient global optimization for conceptual rainfall-runoff models, Water Resour. Res., 28(4), 1015-1031, https://doi.org/10.1029/91WR02985, 1992.

Duan, Q., Schaake, J., Andreassian, V., Franks, S., Goteti, G., Gupta, H. V., Gusev, Y. M., Habets, F., Hall, A., Hay, L., Hogue, T., Huang, M., Leavesley, G., Liang, X., Nasonova, O. N., Noilhan, J., Oudin, L., Sorooshian, S., Wagener, T., and Wood, E. F.: Model parameter estimation experiment (MOPEX): an overview of science strategy and major results from the second and third workshops, J. Hydrol., 320, 3-17, https://doi.org/10.1016/j.jhydrol.2005.07.031, 2006.

Fan, Y., Miguez-Macho, G., Weaver, C. P., Walko, R., and Robock, A.: Incorporating water table dynamics in climate modeling: 1. Water table observations and equilibrium water table simulations, J. Geophys. Res., 112, D10125, doi:10.1029/2006JD008111, 2007.

Farmer, D., Sivapalan, M., and Jothityangkoon, C.: Climate, soil, and vegetation controls upon the variability of water balance in temperate and semiarid landscapes: Downward approach to water balance analysis, Water Resour. Res., 39(2), 1035, https://doi.org/10.1029/2001WR000328, 2003.

Fu, B. P.: On the calculation of the evaporation from land surface [in Chinese]. Sci. Atmos. Sin. 5, 23–31, 1981.

Fu, J. and Wang, W.: On the lower bound of Budyko curve: The influence of precipitation seasonality, J. Hydrol., 570, 292– 303, https://doi.org/10.1016/j.jhydrol.2018.12.062, 2019.

Gao, H., Hrachowitz, M., Schymanski, S. J., Fenicia, F., Sriwongsitanon, N., and Savenije, H. H. G.: Climate controls how ecosystems size the root zone storage capacity at catchment scale, Geophys. Res. Lett., 41, 7916-7923, https://doi.org/10.1002/2014GL061668, 2014.

Gao, H., Hrachowitz, M., Sriwongsitanon, N., Fenicia, F., Gharari, S., and Savenije, H. H.: Accounting for the influence of vegetation and landscape improves model transferability in a tropical savannah region, Water Resour. Res., 52(10), 7999-8022, https://doi.org/10.1002/2016WR019574, 2016.

Gao, H., Birkel, C., Hrachowitz, M., Tetzlaff, D., Soulsby, C., and Savenije, H. H.: A simple topography-driven and calibration-free runoff generation module, Hydrol. Earth Syst. Sci., 23, 787-809, https://doi.org/10.5194/hess-23-787-2019, 2019.

Gentine, P., D'Odorico, P., Lintner, B. R., Sivandran, G., and Salvucci, G.: Interdependence of climate, soil, and vegetation as constrained by the Budyko curve, Geophys. Res. Lett., 39, L19404, https://doi.org/10.1029/2012GL053492, 2012.

Gerrits, A. M. J., Savenije, H. H. G., Veling, E. J. M., and Pfister, L.: Analytical derivation of the Budyko curve based on rainfall characteristics and a simple evaporation model, Water Resour. Res., 45, W04403, https://doi.org/10.1029/2008WR007308, 2009.

Hargreaves, G. H. and Samani, Z. A.: Reference crop evapotranspiration from temperature, Appl. Eng. Agric., 1(2), 96-99, doi: 10.13031/2013.26773, 1985.

Hickel, K. and Zhang, L.: Estimating the impact of rainfall seasonality on mean annual water balance using a top-down approach, J. Hydrol., 331(3-4), 409-424, https://doi.org/10.1016/j.jhydrol.2006.05.028, 2006.

Homer, C. G., Dewitz, J. A., Yang, L., Jin, S., Danielson, P., Xian, G., Coulston, J., Herold, N. D., Wickham, J. D., and Megown, K.: Completion of the 2011 National Land Cover Database

for the conterminous United States-Representing a decade of land cover change information, Photogramm. Eng. Rem. S., 81(5), 345-354, 2015.

Huang, M., Liang, X., and Liang, Y.: A transferability study of model parameters for the variable infiltration capacity land surface scheme, J. Geophys. Res., 108(D22), 8864, https://doi.org/10.1029/2003JD003676, 2003.

Jothityangkoon, C., Sivapalan, M., and Farmer, D. L.: Process controls of water balance variability in a large semi-arid catchment: downward approach to hydrological model development, J. Hydrol., 254(1-4), 174-198, https://doi.org/10.1016/S0022-1694(01)00496-6, 2001.

Konapala, G., and Mishra, A. K. : Three-parameter-based streamflow elasticity model: Application to MOPEX basins in the USA at annual and seasonal scales., Hydrol. Earth Syst. Sci., 20, 2545-2556, https://doi.org/10.5194/hess-20-2545-2016.

Li, H. Y., Sivapalan, M., Tian, F., and Harman, C.: Functional approach to exploring climatic and landscape controls of runoff generation: 1. Behavioral constraints on runoff volume, Water Resour. Res., 50, 9300-9322, https://doi.org/10.1002/2014WR016307, 2014.

Li, D., Pan, M., Cong, Z., Zhang, L., and Wood, E. Vegetation control on water and energy balance within the Budyko framework, Water Resour. Res., 49, 969-976, https://doi.org/10.1002/wrcr.20107, 2013.

Li, D.: Assessing the impact of interannual variability of precipitation and potential evaporation on evapotranspiration, Adv. Water Resour., 70, 1-11, https://doi.org/10.1016/j.advwatres.2014.04.012, 2014.

Maidment, D. R. (Ed.): ArcHydro: GIS for Water Resources, ESRI Press, Redlands, Calif., 2002.

Milly, P. C. D.: Climate, soil water storage, and the average annual water balance, Water Resour. Res., 30(7), 2143-2156, https://doi.org/10.1029/94WR00586, 1994.

Moore, R. J.: The probability-distributed principle and runoff production at point and basin scales, Hydrolog. Sci. J., 30(2), 273-297, https://doi.org/10.1080/02626668509490989, 1985.

Pike, J. G.: The estimation of annual runoff from meteorological data in a tropical climate, J. Hydrol., 12, 2116–2123, https://doi.org/10.1016/0022-1694(64)90022-8, 1964.

Porporato, A., Daly, E., and Rodriguez-Iturbe, I.: Soil water balance and ecosystem response to climate change, Am. Nat., 164(5), 625–632, https://doi.org/10.1086/424970, 2004.

Sankarasubramanian, A., and Vogel, R. M.: Annual hydroclimatology of the United States, Water Resour. Res., 38(6), 1083, https://doi.org/10.1029/2001WR000619, 2002.

SCS.: Hydrology, National Engineering Handbook, Supplement A, Section 4, Chapter 10. Soil Conservation Service, US Department of Agriculture, Washington, DC., 1972.

Shao, Q., Traylen, A., and Zhang, L.: Nonparametric method for estimating the effects of climatic and catchment characteristics on mean annual evapotranspiration, Water Resour. Res., 48, W03517, https://doi.org/10.1029/2010WR009610, 2012.

Tang, Y. and Wang, D.: Evaluating the role of watershed properties in long-term water balance through a Budyko equation based on two-stage partitioning of precipitation, Water Resour. Res., 53, 4142–4157, https://doi.org/10.1002/2016WR019920, 2017.

Troch, P., Loon, E. V., and Hilberts, A.: Analytical solutions to a hillslope-storage kinematic wave equation for subsurface flow, Adv. Water Resour., 25(6), 637-649, https://doi.org/10.1016/S0309-1708(02)00017-9, 2002.

Troch, P. A., Carrillo, G., Sivapalan, M., Wagner, T., and Sawicz, K.: Climate-vegetation-soil interactions and long-term hydrologic partitioning: Signatures of catchment co-evolution, Hydrol. Earth Syst. Sci., 17, 2209-2217, https://doi.org/10.5194/hess-17-2209-2013, 2013.

Turc, L.: Le bilan d'eau des sols: Relation entre les precipitations, l'evaporation et l'ecoulement, Ann. Agron., Serie A 5, 491–595, 1954.

USDA: Gridded Soil Survey Geographic (gSSURGO) Database User Guide, U. S. Dep. of Agric., Nat. Resour. Conserv. Serv., Washington, D. C., 2014.

Wang, D. and Hejazi, M.: Quantifying the relative contribution of the climate and direct human impacts on mean annual streamflow in the contiguous United States, Water Resour. Res., 47, W00J12, https://doi.org/10.1029/2010WR010283, 2011.

Wang, D. and Tang, Y.: A one-parameter Budyko model for water balance captures emergent behavior in Darwinian hydrologic models, Geophys. Res. Lett., 41, 4569–4577, https://doi.org/10.1002/2014GL060509, 2014.

Wang, D.: A new probability density function for spatial distribution of soil water storage capacity leads to SCS curve number method, Hydrol. Earth Syst. Sci., 22, 6567-6578, https://doi.org/10.5194/hess-22-6567-2018, 2018.

Wood, E. F., Lettenmaier, D. P., and Zartarian, V. G.: A land-surface hydrology parameterization with subgrid variability for general circulation models, J. Geophys. Res., 97(D3), 2717-2728, https://doi.org/10.1029/91JD01786, 1992.

Woods, R.: The relative roles of climate, soil, vegetation and topography in determining seasonal and long-term catchment dynamics, Adv. Water Resour. Res., 37, 701-708, https://doi.org/10.1016/S0309-1708(02)00164-1, 2003.

Xing, W., Wang, W., Shao, Q., and Yong, B.: Identification of dominant interactions between climatic seasonality, catchment characteristics and agricultural activities on Budyko-type equation parameter estimation, J. Hydrol., 556, 585-599, https://doi.org/10.1016/j.jhydrol.2017.11.048, 2018.

565 Yang, H., Yang, D., Lei, Z., and Sun, F.: New analytical derivation of the mean annual water-
566 energy balance equation, Water Resour. Res., 44, W03410,
567 https://doi.org/10.1029/2007WR006135, 2008.
568 Yao, L., Libera, D., Kheimi, M., Sankarasubramanian, A., and Wang, D.: The roles of climate
569 forcing and its variability on streamflow at daily, monthly, annual, and long-term scales,
570 Water Resour. Res., https://doi.org/10.1029/2020WR027111, 2020.
571 Yokoo, Y., Sivapalan, M., and Oki, T.: Investigating the roles of climate seasonality and landscape
572 characteristics on mean annual and monthly water balances, J. Hydrol., 357(3-4), 255-269,
573 https://doi.org/10.1016/j.jhydrol.2008.05.010, 2008.
574 Zhang, L., Dawes, W. R., and Walker, G. R.: Response of mean annual evapotranspiration to
575 vegetation changes at catchment scale, Water Resour. Res., 37, 701–708,
576 https://doi.org/10.1029/2000WR900325, 2001.
577 Zhao, R. J.: The Xinanjiang model applied in China, J. Hydrol., 135(1–4), 371–381,
578 https://doi.org/10.1016/0022-1694(92)90096-E, 1992.
579

Table 1: The USGS gage stations, climate aridity index, the estimated potential maximum retention of curve number method (S_{CN}), and the average soil water storage capacity (S_b) for the study watersheds.

Index	Station Name	State	USGS Gauge Number	Climate Aridity Index	S_{CN} (mm)	S_b (mm)
1	Susquehanna River	NY	01503000	0.69	100	862
2	Chemung River	NY	01531000	0.84	95	518
3	Juniata River	PA	01567000	0.85	134	714
4	Rappahannock River	VA	01668000	0.85	152	792
5	Yadkin River	NC	02116500	0.71	153	1221
6	Chattahoochee River	GA	02339500	0.69	182	1559
7	Escambia River	FL	02375500	0.73	143	1075
8	Allegheny River	NY	03011020	0.68	153	1369
9	New River	VA	03168000	0.69	177	1494
10	Great Miami River	OH	03274000	0.89	63	301
11	Eel River	IN	03328500	0.92	68	304
12	East Fork White River	IN	03364000	0.83	68	378
13	Little Wabash River	IL	03381500	0.96	68	279
14	Fox River	WI	04073500	1.12	162	520
15	Auglaize River	OH	04191500	0.98	56	225
16	Maquoketa River	IA	05418500	1.19	72	209
17	Wapsipinicon River	IA	05422000	1.16	69	210
18	Rock River	WI	05430500	1.11	98	316
19	Pecatonica River	IL	05435500	1.11	66	214
20	Kishwaukee River	IL	05440000	1.03	70	255
21	Green River	IL	05447500	1.10	75	247
22	Iowa River	IA	05454500	1.18	65	191
23	Cedar River	IA	05458500	1.17	65	193
24	Kankakee River	IL	05520500	0.93	101	448
25	Fox River	IL	05552500	1.04	88	321
26	Spoon River	IL	05570000	1.12	71	227
27	Kaskaskia River	IL	05592500	0.99	67	263
28	Blue River	KS	06884400	1.70	74	127
29	Thompson River	MO	06899500	1.16	65	195
30	Meramec River	MO	07019000	0.95	109	460
31	Chikaskia River	OK	07152000	1.82	77	121
32	Neosho River	KS	07183000	1.42	63	140
33	Deep Fork River	OK	07243500	1.40	87	197
34	Neches River	TX	08033500	1.14	174	540
35	Elm Fork Trinity River	TX	08055500	1.63	87	159

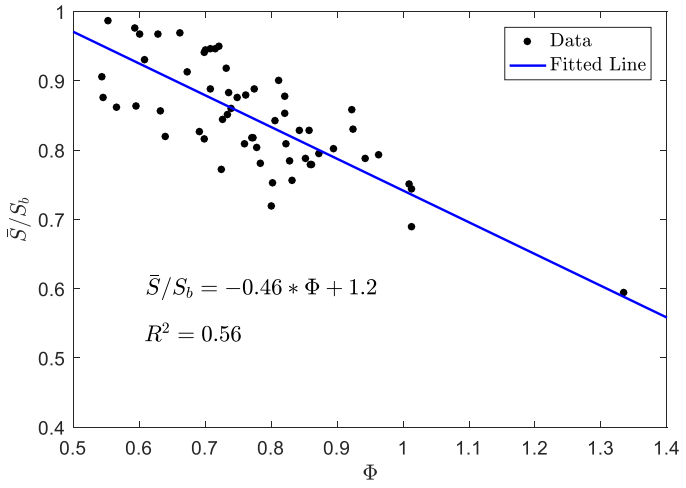

585

586 Figure 1: The degree of saturation $\left(\frac{\bar{S}}{S_b}\right)$ under long-term average climate versus climate aridity
587 index (Φ).

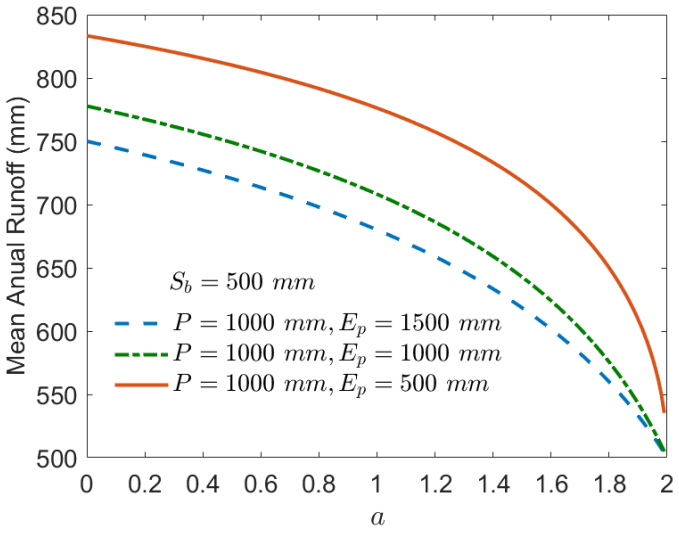

588

589 Figure 2: The sensitivity of mean annual runoff (Q) to the value of shape parameter (a).

590

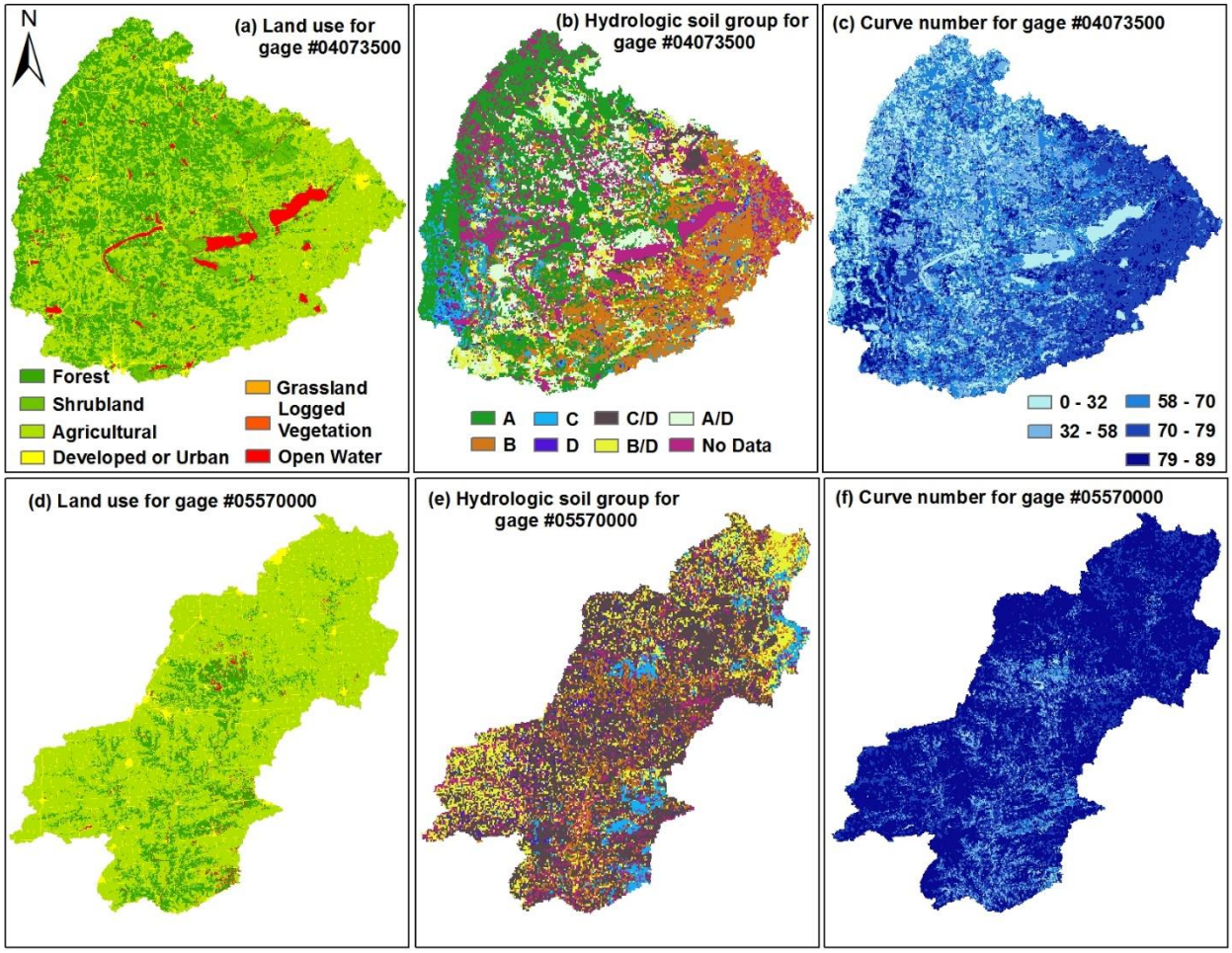

Figure 3: The spatial distribution of land use and land cover for Fox River watershed in Wisconsin (a) and Spoon River watershed in Illinois (d), the hydrologic soil groups for Fox River watershed (b) and Spoon River watershed (e), and the curve numbers for Fox River watershed (c) and Spoon River watershed (f).

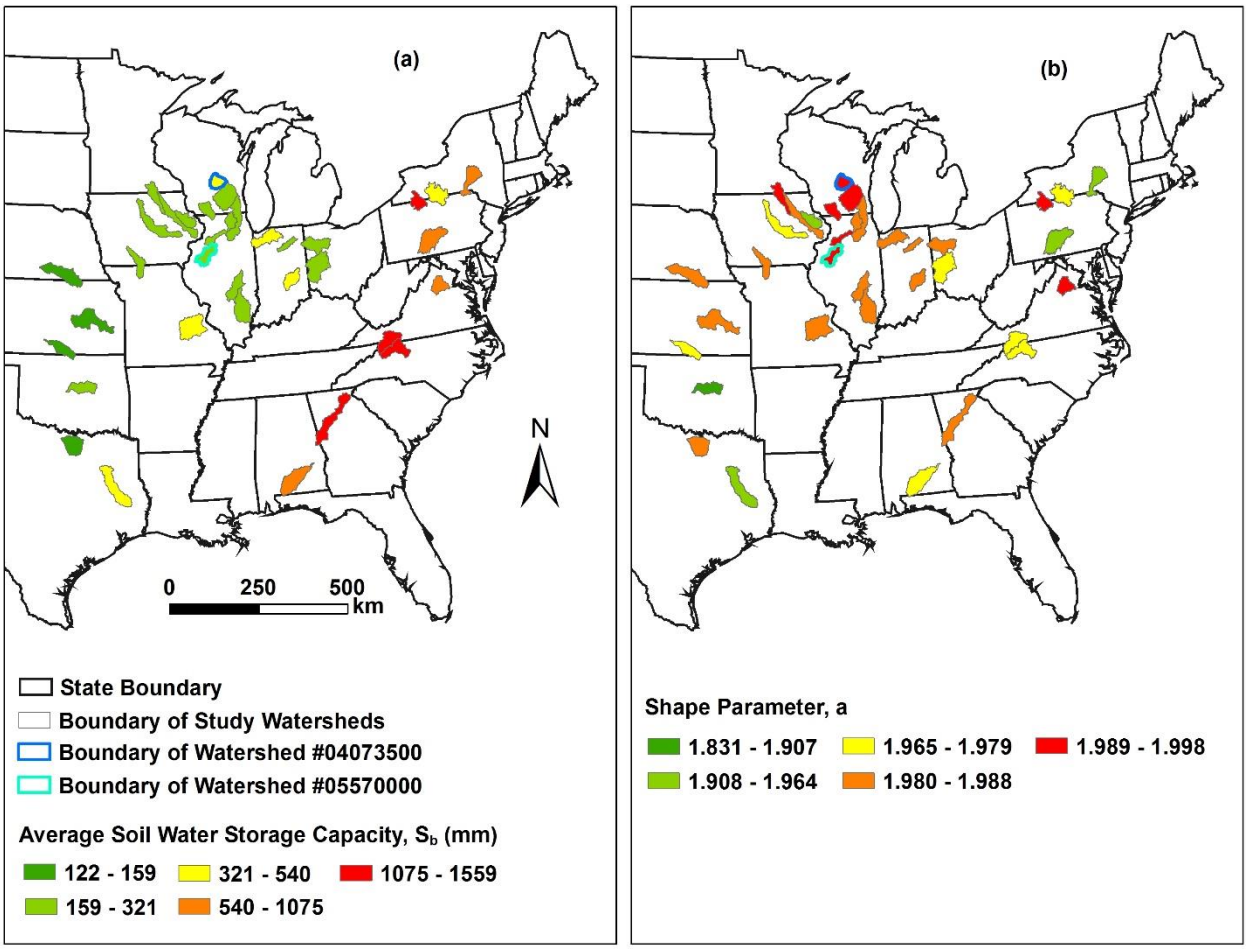

Figure 4: The estimated average soil water storage capacity (S_b) as a function of S_{CN} and climate aridity index (a) and shape parameter from soil data (b).

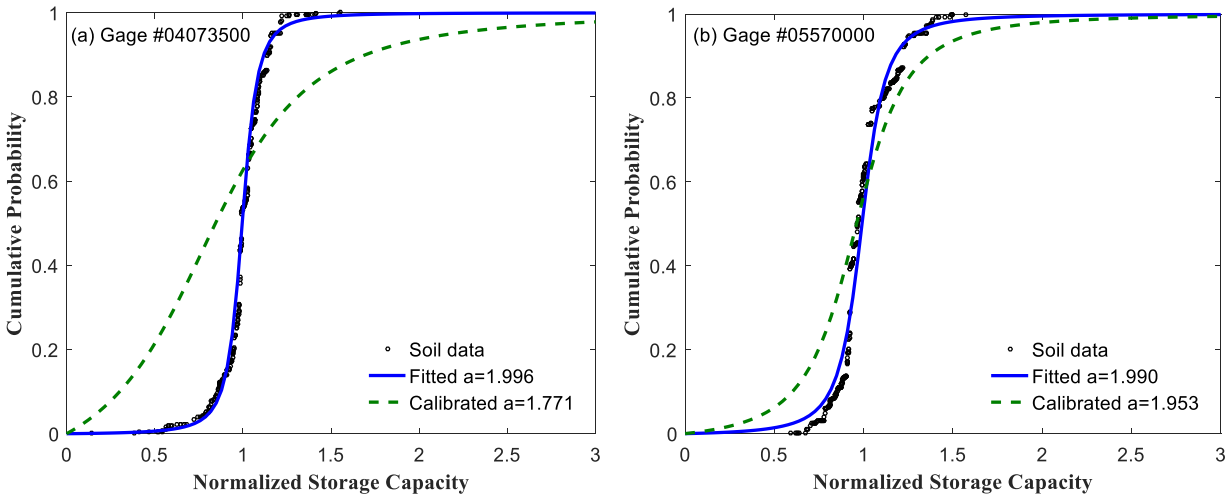

601

602 Figure 5: The estimated shape parameter for the spatial distribution of soil water storage capacity
603 based on soil data and the calibrated shape parameter based on mean annual water balance in the
604 Fox River watershed (a) and the Spoon River watershed (b).

605

606

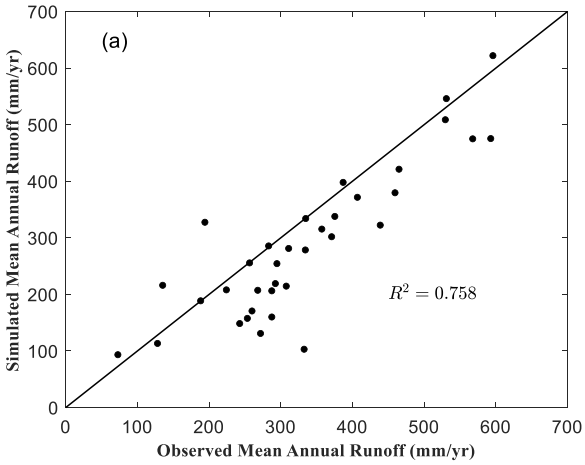

607

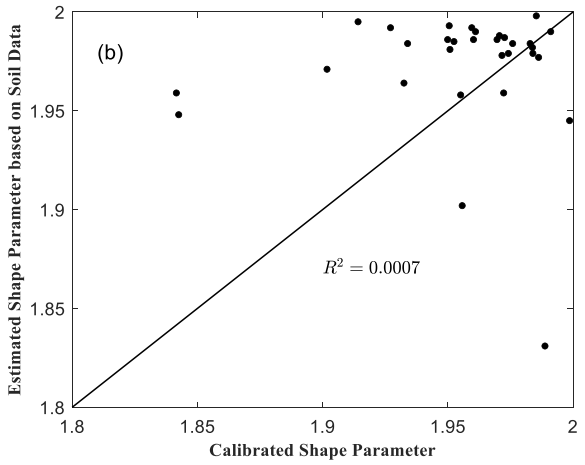

608

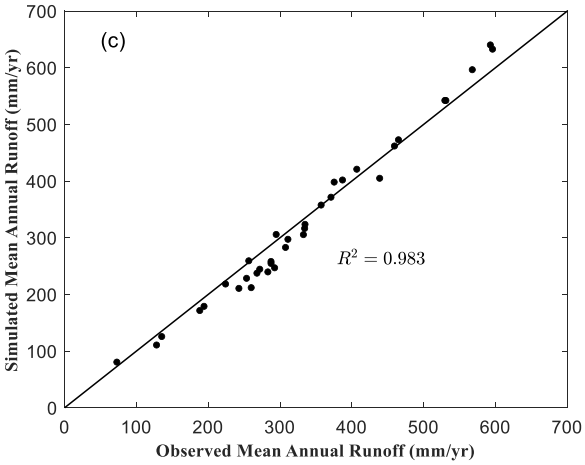

609 Figure 6: (a) Observed versus simulated mean annual runoff using shape parameter based on
610 soil data; (b) Soil data-based versus calibrated shape parameter; and (c) Observed versus
611 simulated mean annual runoff using shape parameter based on calibration.

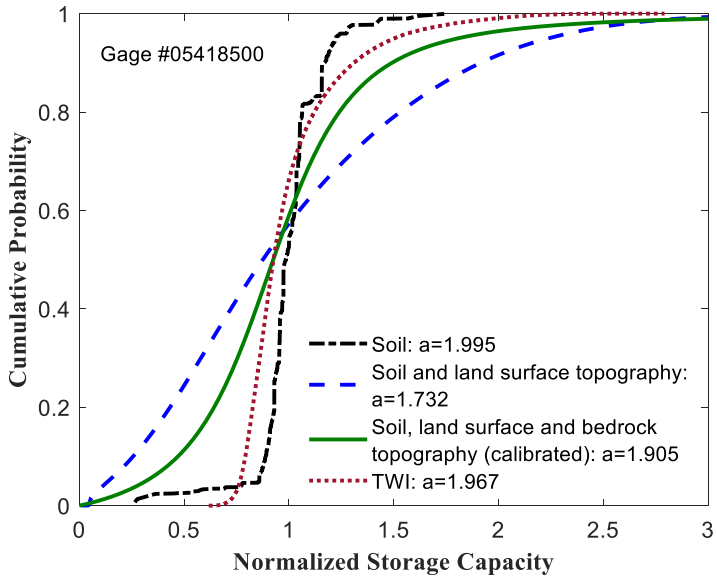

Figure 7: The effects of soil, land surface topography, bedrock topography, and topographic wetness index (TWI) on the shape parameter of the spatial distribution of soil water storage capacity.